Minireviews
doi.org/10.1002/batt.202000258

Chemistry Europe
European Chemical Societies Publishing

Special Collection

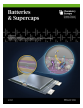

# Understanding the Nature of Solid-Electrolyte Interphase on Lithium Metal in Liquid Electrolytes: A Review on Growth, Properties, and Application-Related Challenges

Maryam Nojabaee,*[a] Dennis Kopljar,[a] Norbert Wagner,[a] and Kaspar Andreas Friedrich[a, b]

A stable solid-electrolyte interphase (SEI) is of crucial essence for realization of lithium (Li) metal batteries. This article provides an overview of attempts undertaken to understand the nature of the natural SEI, including growth behavior at the open circuit potential and under cycling conditions as well as underlying causes of instabilities. Additionally, the influence of features such as morphology and composition of the SEI and electrolyte properties on the charge transport and transfer mechanism, resulting in distinct growth behavior and overall stability, is elaborated. Finally, it will be discussed how already at the fundamental stage of research, it is crucial to take into account the implications that progressing from coin-cell level to more realistic cell and cycling conditions has on SEI properties and stability.

## 1. Introduction

Batteries are a key technology for the future energy system and an important enabler for the decarbonization of society. The high energy density of Li-ion batteries (LIB), along with the continuously decreasing cost as well as the long cycle-life of these systems facilitate their integration into a vast variety of applications in the field of portable devices, the electrification of transport and stationary energy storage.[1] However, as LIB will inevitably reach their theoretical energy density limit, new cell chemistries are under intensive investigation. One pathway is the implementation of high capacity anodes of which Li metal is considered the most promising.[2] Due to the high gravimetric and volumetric capacity of Li metal (3860 $mAh\,g^{-1}$ and 2061 $mAh\,cm^{-3}$) and the lowest electrode potential (−3.04 V vs. the standard hydrogen electrode) at hand, this development step will enable a significant increase in energy density while simultaneously paving the way for the next generation of Li-metal-based cell chemistries, i.e. Li-sulfur, solid-state and, in the longer term, Li-air batteries.[3]

The challenges, advances and strategies for the successful application of Li metal are summarized in numerous recent review articles.[4] The most challenging issues on the material level are the infinite volume change of Li upon cycling and its highly reducing nature which leads to the continuous decomposition of electrolyte on the metal surface. In modern state-of-the-art graphite anodes, a relatively stable SEI forms after the first cycles, while further growth is decelerated by the insulating nature of this SEI layer.[5] The SEI on the graphite appears to grow further at higher current densities resulting in capacity fade.[6] This is even more critical in the case for Li metal where the initial SEI layer without dedicated electrolyte design falls short of shielding the Li metal from the electrolyte due to its continuous disintegration and crack formation upon cycling, constantly exposing fresh metallic Li to the electrolyte. As a result, this leads to low Coulomb efficiency (CE) and, eventually, low cycle life. For a Li metal cell to ensure comparable cycle life to current LIB, a CE of $>99.9\%$ needs to be achieved which translates into a cycle number $>2000$ before 80% of initial Li inventory is lost.[7] This imposes strict requirements towards the protection of the interface between Li and the electrolyte as well as the stability of this interface layer. In that respect, another closely related key challenge for safe operation of Li metal cells is the formation and growth of Li dendrites which is a result of inhomogeneous stripping and plating behavior already at moderate current densities. Accordingly, as the morphological and compositional properties of the interface and the corresponding transport properties strongly influence the deposition of Li ions, the SEI plays a critical role in extending the operational range to practical current densities before dendrite growth becomes an issue. For a more elaborate discussion on this topic, it is referred to the considerable work contributing to the most recent understanding of this phenomenon.[8]

To allow for a rational development of a dedicated SEI in liquid electrolytes that is capable of solving the above challenges, first, a clear understanding of the complex nature of the individual SEI components and the morphology of the layer as function of the operating conditions is required. In a second step, insights into the role of the components and the

[a] Dr. M. Nojabaee, D. Kopljar, Dr. N. Wagner, Prof. Dr. K. A. Friedrich
Department of Electrochemical Energy Technology
Institute of Engineering Thermodynamics
Pfaffenwaldring 38–40, 70569 Stuttgart, Germany
E-mail: Maryam.nojabaee@dlr.de
[b] Prof. Dr. K. A. Friedrich
Institute for Building Energetics,
Thermotechnology and Energy Storage
University of Stuttgart
Pfaffenwaldring 31, 70569 Stuttgart, Germany

Special Collection An invited contribution to a Special Collection on Lithium Metal Anode Processing and Interface Engineering



 

factors that are desired or must be avoided for a functioning and stable interphase layer have to be established. While this knowledge has been created and refined for graphite anodes over decades, there is still a lack of understanding on the nature and the properties of the SEI on Li metal, the Li ion transport through this layer and how this effects SEI ability to shield the metal from the electrolyte and suppress dendrite formation. That said there is a considerable number of review papers available exploring the materials and designs for an artificial SEI and tuning the natural SEI to improve cell performance and suppress dendrite formation.[9] In this contribution, we intend to provide an overview of attempts on understanding the nature of the natural SEI, including growth behavior at the open circuit potential and cycling conditions as well as causes of instabilities, potentially being of value for the design of artificial SEI and to aid in closing this gap by stimulating research on these critical aspects. Finally, it will be discussed how already at a fundamental stage of research and when trying to solve the above challenges on coin-cell level it is important to keep in mind the implications when switching towards more practical conditions and cells which more closely resemble application. Otherwise although being of high academic value, their informational merit is limited when it comes to using that knowledge for producing long-term stable and efficient Li metal cells.

## 2. The Nature of the Solid-Electrolyte Interphase (SEI)

Thermodynamically most metals undergo decomposition exposed to an oxidizing environment. Nonetheless, metals essentially indicate surface property of passivity, rendering their application as structural materials. The thin passivating film on the surface decelerates the degradation processes shielding the underlying metal. The passivation either stabilizes once the formed film is thermodynamically in equilibrium with the electrolyte, or the kinetics of cation transfer from the resulting film to the electrolyte is sufficiently sluggish that the dissolution current becomes insignificant and thereby protecting the metal, while the passivating layer is not yet in dissolution equilibrium. The passivation current density depends on the electrode potential, explained by an increase in the oxidation state of the cations at the surface of the layer resulting in a variation in the composition of the passivating film with the potential.[10]

In the case of Li metal, Li is unstable in almost any environment and in exposure to almost all potential electrolytes as a result of its highly positive passivation potential. Indeed, Li has been shown to be susceptible to degradation even attempted to be preserved in an inert environment. The pristine Li surface exhibits impurities of the oxide and carbonate decorating the grain boundaries.[11] Therefore, here firstly the formation and growth of the passivation film on Li metal in contact with liquid electrolyte at the open circuit potential (OCP) will be discussed.

### 2.1. SEI Growth on Li Metal in Contact with Electrolyte at the Open Circuit Potential (OCP)

#### *2.1.1. Short-Term Growth*

The growth of thin oxide layers (thickness of 10–20 nm) forming on the metal surface with respect to time has been reported in literature to undergo a direct/inverse-logarithmic, parabolic or linear behavior.[12] Linear growth for the early stages of film formation on the Li surface exposed to glyme-based solid-liquid composite electrolytes was observed and discussed.[13] The linear growth of oxide on metal surface is found for metals with porous or cracked oxide film where the ion transfer takes place at higher rate than the chemical reaction. The surface chemistry of preserved pristine Li

Dr. Maryam Nojabaee completed her Ph.D. in chemistry at Max-Planck-Institute for solid-state research in 2018. Since then, she works at the German Aerospace Center (DLR), department of Electrochemical Energy Technology as a scientist and her research focuses on the next-generation batteries specifically metal-sulfur batteries.

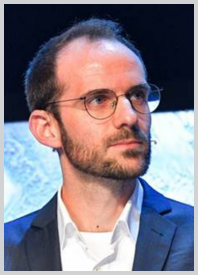

Dennis Kopljar is a research scientist at the German Aerospace Center (DLR) with a background in chemical engineering and electrochemistry. His research interests evolve around the development and characterization of electrochemical processes and technologies for energy storage and electrification of the chemical industry. His current work is mostly dedicated to lithium-ion and next-generation batteries as well as electrochemical reduction of $CO_2$.

Dr. Norbert Wagner (Ph.D. in Chemistry) is the leader of the battery technology group at the department of Electrochemical Energy Technology at the German Aerospace Center (DLR) since 2011. Since 1985 he is working in the field of electrochemistry specifically fuel cells, Li-ion batteries, metal-sulfur, and metal-air batteries.

Prof. Dr. Kaspar Andreas Friedrich is head of the department Electrochemical Energy Technology at the German Aerospace Center (DLR), Institute of Engineering Thermodynamics since 2004. He is also professor at the University of Stuttgart, faculty of Energy-, Process- and Bio-Technology. He completed his PhD at Fritz-Haber Institute of the Max-Planck-Society in physical chemistry in 1989.

displaying the native passivation film, which mainly decorates the grain boundaries as opposed to a dense homogeneous non-porous film, corroborates this experimentally recoded linear time-response of SEI growth during initial contact. This leads to a surface reaction-controlled reaction rather than a diffusion dominant process. The time-dependence of film growth yields a linear response for surface-controlled growth mechanisms given as [Eq. (1)]:[13]

$$L_{\text{SEI, short}} = (s\Delta\mu_{\text{Li}})t \quad (1)$$

where s is the reaction constant and $\Delta\mu_{\text{Li}}$ is difference in the chemical potential of the Li over the formed film. This rate law holds for the formation of a porous oxide layer up to any thickness as long as the porosity enables the electrolyte to access to the reaction front.

Among reported growth rate laws, quite often the growth of the thinner oxide film is characterized by logarithmic rate.[14] Here, the electric field created by the tunneling of electrons from the metal to oxidizing species at the oxide surface accelerates the sluggish ion transport across the film by enhancing the defect injection rate at the interface (metal/film or film/electrolyte). The model is essentially based on the quantum mechanical tunneling where an electron can overcome an energy barrier in the absence of thermal activation. An electric field between the oxide surface and the metal is induced by penetration of the electron through an energy barrier which causes a shift in the Fermi level across the layer and reduces the activation energy of charge transfer, resulting in further growth. However, this growth behavior is self-limiting, meaning the induced field decreases as the oxide grows and is eventually lowered to values that are no longer adequate for the necessary ion movement. The model implies that growth here occurs only when strong electric fields are present for ultra-thin films and is consequently only relevant for early stages of passivation. To our knowledge the logarithmic growth rate has not been reported for the Li passivation process exposed to the liquid electrolyte. Indeed, in addition to the mentioned linear time-response, the diffusion-controlled growth is what has been quite often used.[15] However, it is important to note that in all the reported studies on Li the SEI shows an initial value of larger than zero indicating that the formation process is essentially started before recording the data. Accordingly, the initial logarithmic growth cannot be completely excluded given the limited initial resolution of the experiment, considering the required time of assembling the cell as well as recording the impedance data. Additionally, the pre-exponential factor and an activation term play a crucial role in determining the growth rate for the initial passivation process, i.e. the primary surface chemistry of Li dictates the initial growth model. Suggestively, the SEI on the preserved pristine Li handled in an inert environment tends to indicate initial linear or logarithmic growth, as opposed to the situation where the native passivation film grows to a non-porous film covering the entire surface, where observation of such growth behavior is indeed no longer possible. The crucial operational implication is to note the influence of the prime surface chemistry of Li on the formation, growth and stability of this layer. In this respect, the chemical or mechanical pre-treatment of pristine Li proposed in the literature could be an integral step to eliminate the impurities and implement reproducible baseline condition.[11,16]

### 2.1.2. Long-Term Growth (OCP)

Upon the transition from separate island growth to a thick non-porous film, the kinetics of the process are observed to undergo a change from linear to parabolic behavior.[12] In Wagner theory which is commonly employed for describing the growth of thicker oxides, further oxidation is limited by the chemical diffusion through the oxide due to the negligible field effects.[17] Here, the growth indicates a parabolic rate law, where the transport of charged species is essentially based on the linear diffusion equation and is related to the defect structure of the oxide film. Considering the Fick's first law, the flux of Li ($j_{\text{Li}}$) as the neutral species is given by [Eq. (2)]:

$$j_{Li} = -D_{Li}c_{Li}\frac{\partial\eta_{Li}}{\partial x} \quad (2)$$

where $c_{\text{Li}}$ refers to the concentration of Li and $\eta_{\text{Li}}$ the electrochemical potential of Li given by $\eta_{\text{Li}} = \mu_{\text{Li}} + zF\varphi$. The ion flux here is established either by the ambipolar diffusion ($D_{\text{Li}}$) of cation ($Li^+$) and electron (eon), further from the anode towards the electrolyte or by the diffusion of the anion in the reverse direction depending on the defect chemistry and electronic structure of the oxide. By extension, the ambipolar diffusion for the growing film on metal in contact with the liquid electrolyte could be illustrated as Figure 1, where $\mu_{\text{Li}}$ is the chemical potential of the Li. The difference between $\mu_{\text{Li}}(Li)$ in the film in equilibrium with metal and $\mu_{\text{Li}}(el)$ in the oxide film in equilibrium with the liquid electrolyte gives the chemical potential difference of the metal across the film ($\Delta\mu_{\text{Li}}$). For

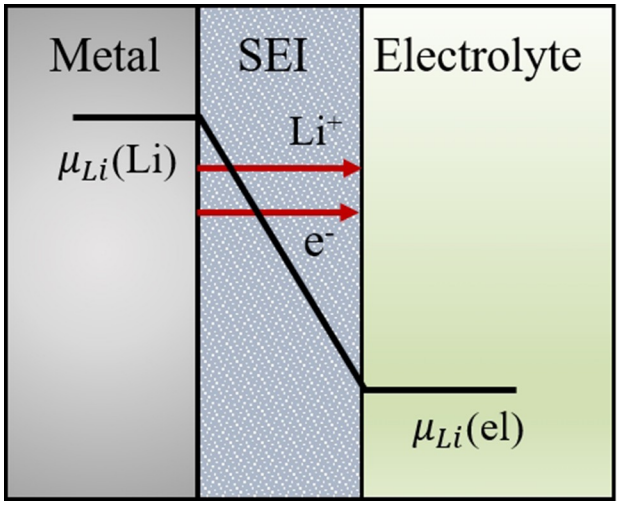


**Figure 1.** Ambipolar diffusion of ions and electrons as well as the chemical potential gradient in a growing film on metal.

simplicity, it is presumed that the SEI is composed of one inorganic compound.

Based on this assumption and definition of binary interdiffusion, the flux of Li across the film is further driven as [Eq. (3)]:[18]

$$j_{Li} = -\frac{1}{4F^2}\sigma_{Li}^{\delta}\nabla\mu_{Li} = -\frac{1}{4F^2}\sigma_{Li}^{\delta}\frac{\Delta\mu_{Li}}{L_{SEI}} \quad (3)$$

where $F$ is the Faraday constant. The chemical potential gradient ($\nabla\mu_{\mathrm{Li}}$) is approximated by the difference of the chemical potential ($\Delta\mu_{\mathrm{Li}}$) of Li over the film. Here, the kinetic factor of ambipolar conductivity is given by [Eq. (4)]:

$$\sigma_{Li}^{\delta} = \frac{\sigma_{Li+}\sigma_{eon}}{(\sigma_{Li+} + \sigma_{eon})} \quad (4)$$

which is expressed by the partial conductivities of ions $\sigma_{\mathrm{Li}+}$ and electrons $\sigma_{\mathrm{eon}}$.

Additionally, the rate of the reaction is inversely proportional to the thickness ($L$) which is related to the flux of the ions. This is represented as [Eq. (5)]:

$$j_{Li}\, v_{SEI} = \frac{dL}{dt} = \frac{k_p}{L} \quad (5)$$

here $k_p$ is parabolic reaction rate constant and $v_{\mathrm{SEI}}$ is molar volume of SEI. Combining Equations (3) and (5) the thickness of the film yields as:

$$L_{SEI,\,long} = k_p(t)^{0.5} \quad (6)$$

where $k_{\mathrm{p}}$ is given by [Eq. (7)]:

$$k_p = -\frac{V_m}{F^2}\int \sigma_{Li}^{\delta} d\mu_{Li} \quad (7)$$

Unlike the short-term growth rate of the SEI layer where the differences are noticeable in recorded data on the graphite anode and Li metal as well as in Li metal itself in contact with liquid and solid electrolyte, the parabolic growth rate of the SEI layer in longer times has been reported for all of these systems analogously.

For the SEI formed on Li metal in contact with the solid electrolyte, Wenzel et al. rewrote the Equations (6) and (7) based on electronic and the ionic conductivities to derive the resistance of the SEI ($R$) according to[Eq. (8)]:[19]

$$R(t) = \frac{1}{A\sigma_{SEI}}\cdot\left(\frac{2M_{SEI}\sigma_{eon}\sigma_{Li^+}\mu_{Li}^{\circ}}{F^2\rho_{SEI}x(\sigma_{eon}+\sigma_{Li^+})}\right)^{0.5}(t)^{0.5} = k_p(t)^{0.5} \quad (8)$$

here $M_{\mathrm{SEI}}$ and $\rho_{\mathrm{SEI}}$ are the molar mass and density of the SEI, respectively. Additionally, $t$ is the SEI growth time, $x$ a stoichiometric factor, $\mu_{\mathrm{Li}}^{\circ}$ the chemical potential of pure Li metal and $A$ the macroscopic electrode area. The authors further revisit the equation 8 for an ideal SEI where the electronic conductivity is negligible enough ($\sigma_{\mathrm{eon}} \ll \sigma_{\mathrm{ion}}$) as [Eq. (9)]:

$$R(t) = \frac{\sigma_{eon}^{0.5}}{A\sigma_{Li^+}}\cdot\left(\frac{2M_{SEI}\mu_{Li}^{\circ}}{F^2\rho_{SEI}x}\right)^{0.5}(t)^{0.5} = k_p(t)^{0.5} \quad (9)$$

For the SEI formed in liquid electrolyte this assumption should be taken with more caution, as commonly cracks and certain porosity exist inside the SEI layer with considerable presence of the liquid electrolyte and organic phases. This simplification however could still hold true to some extent, for the systems indicating a bilayer structure of SEI on the Li metal exposed to liquid electrolyte (see sections 2.2 and 3.2) with the presence of a non-porous dense inorganic inner layer of at least 20–30 nm.[20]

### 2.2. SEI Evolution upon Cycling and Related Challenges

In contrary to graphite and silicon anodes, the evolution of the SEI on Li metal under cycling condition has so far not been investigated sufficiently.[21] Therefore, in addition to the SEI models available for Li metal anode,an attempt is made herein to address the existing models for the mentioned electrodes and to discuss the applicability of these models for Li metal.

Under an electrical field, in addition to diffusion more complex transport modes such as migration must be considered. Ignoring the convection induced current, the flux ascribed to SEI growth ($i_{\mathrm{SEI}}$) could be defined using migration and diffusion factor described as [Eq. (10)]:

$$i_{\mathrm{SEI}} = -z_{e^-}FD\nabla c_{\mathrm{i}} - \frac{z_{e^-}^2 DF^2}{RT}c_{\mathrm{i}}\nabla\varphi \quad (10)$$

where F is the Faraday constant and $R$ universal gas constant, $D$ is the ambipolar diffusion, $c_{\mathrm{i}}$ the concentration of charge carrier in SEI and $\nabla\varphi$ potential gradient over SEI. Peled discussed the $i_{\mathrm{SEI}}$ for an ideal pure ionic conductive SEI ($t_+ = 1$ where the diffusion induced flux is not present and the migration of cation is the rate-determining step, see Figure 2a.[15a]

Taking into account the migration of ions in a solid crystal under an external field with the assumption that the thickness of the SEI is large enough (greater than the space charge lengths), as well as the electrode overpotential $(\eta)$ induced by the electromigration, for the higher electric field, Peled derived the Tafel-like equation [Eq. (11)]:[15a]

$$i_{\mathrm{SEI}} = i_{\mathrm{SEI}}^{0} e^{(\alpha_{\mathrm{SEI}}ZF\eta/RTL)} \quad (11)$$

where $\alpha_{\mathrm{SEI}}$is the charge transfer coefficient.

A continuous growth of SEI on Li metal has been consistently reported, implying the conduction of anions or electrons across the SEI. Peled assumed for storage conditions, the electron transport through a homogeneous SEI as the rate-limiting factor leading to the derivation of the parabolic rate growth, which did not necessarily corroborate with the experimental observations.[15a] Newman similarly discussed a model that takes into account Li and electron conduction

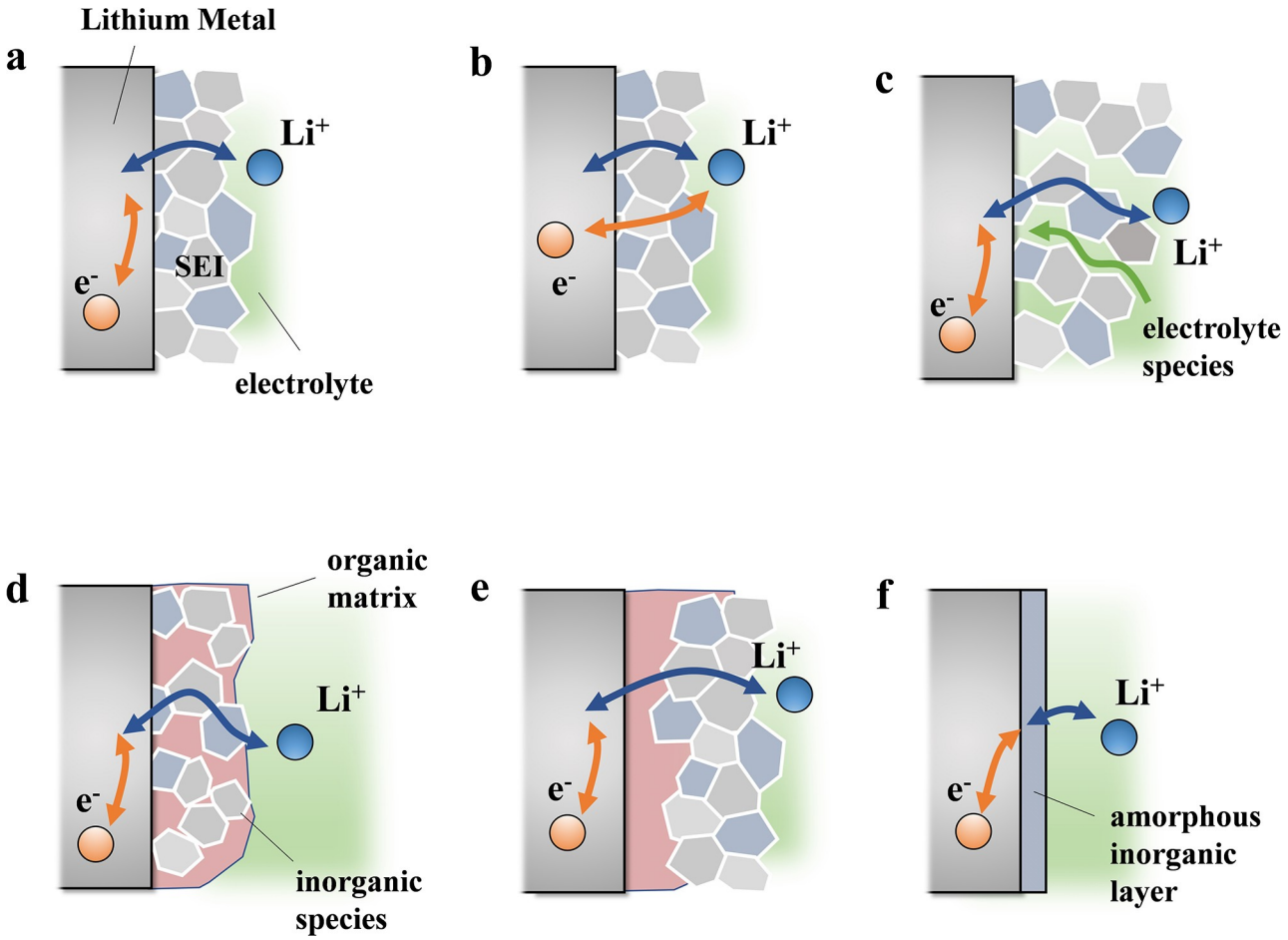


**Figure 2.** Possible morphologies and resulted charge transport across the SEI: a) Purely ionic conductive SEI where the cation-transport through SEI is the rate-determining step. b) Ionic and electronic conductive SEI where the electron-transport is the rate-determining step. Here, there is analogy to the multilayer structure with the inner inorganic and outer organic layer. c) Porous SEI where electrolyte diffusing towards SEI/Li interface is responsible for SEI growth. d) Mosaic structure where inorganic and organic compounds are present from outer to inner layer. e) Multilayer structure with inner-organic and outer-inorganic where the growth mechanism is more complex. f) Monolithic structure composed of thin amorphous inorganic layer.

shown schematically in Figure 2b, which estimated the observed SEI growth.[22] This model however failed to predict the experimentally observed resistance of the SEI on graphite, yielding substantially higher values.

Among more recent studies, Das et al. discussed the growth of the SEI on graphite under cycling condition for a mixed conductor SEI starting from a classical Butler-Volmer equation for the post-first cycles (excluding the first formation cycle) [Eq. (12)]:[23]

$$i = i_{SEI}^{0}\left[e^{(1-\alpha_{SEI})\tilde{\eta}_1} - e^{(-\alpha_{SEI})\tilde{\eta}_1}\right] \quad (12)$$

where $\tilde{\eta}_1$ is the potential drop over the Stern layer at the SEI/electrolyte interface, $\alpha_{SEI}$ is the charge transfer coefficient, $i_{SEI}^{0}$ is the exchange current density for the SEI reaction expressed by the local concentration of mobile electrons ($\tilde{c}_{eon,\,SEI}$) and ions ($\tilde{c}_{Li+,\,SEI}$) according to[Eq. (13)]:

$$i_{SEI}^{0} = k_{SEI}\left(\tilde{c}_{eon,\,SEI}\tilde{c}_{Li+,\,SEI}\right)^{(1-\alpha_{SEI})}\tilde{c}_{SEI}^{\alpha_{SEI}} \quad (13)$$

where $k_{SEI}$ is the rate constant and $\tilde{c}_{SEI}$ the dimensionless SEI concentration. It is proposed that the coupled diffusion and/or migration of electrons from the graphite/SEI interface to the SEI/electrolyte interface is accountable for the reported SEI growth thus the rate-determining step. The model is consistent with experimental results that SEI growth is enhanced upon lithiation while suppressed on delithiation of the graphite anode. This is indeed a crucial issue that is worth investigating and discussing for Li metal anode as well.

These above-mentioned models could potentially be applicable for the SEI behavior in the largely accepted bilayer structure of the SEI on the Li metal with the inner dense inorganic layer and outer porous organic phase whereby the electrolyte diffuse to the inorganic-phase front.[20] However, they might fall short for a real system of Li anode, where porosity in the inorganic phase and mosaic structures have been repeatedly reported.[24]

Alternatively, models exist in the literature in which the electrolyte diffusing towards the electrode interface through a porous SEI accounts for the long-term growth of the SEI, illustrated in Figure 2c.[21c,25] As an example, Safari et al.

developed a multimodal physics-based aging model using the continuous, small-scale growth of an SEI layer on graphite. Herewith, the solvent decomposition kinetics along with the solvent diffusion through the SEI layer were incorporated as the rate-determining factors. It is shown that as opposed to the OCV conditions where the SEI growth proved to be diffusion-limited, at the cycling conditions diffusion-, kinetic-limited as well as mixed regimes were able to be estimated. These models are quite comparable to the mosaic structure depicted in Figure 2d, where the organic and electronically conductive phases are in fact in contact with Li metal.

While we sought here to leverage the existing models for the intercalation electrode to understand the kinetics of SEI growth under cyclic conditions, there are clearly substantial differences between Li metal and intercalation anodes requiring the further development and refining of the existing models. These dissimilarities include the more sophisticated reported morphologies with the amorphous inner layer and the monolithic structure shown in Figure 2e and 2f, respectively, requiring further consideration.[26] In the case of inner organic layer as well as for the mosaic morphology, growth paths induced by electron conduction through the organic phase along with inward transport of organic radicals are conceivable. The underlying factors causing the emergence of different structures and the consequential stripping-plating behaviors is addressed in section 3.2. In addition, the formation of porosity, voids, dendrites, porous and dead-lithium are among the phenomena making intercalation models impractical to predict the SEI evolution on Li metal under cycling. Naturally, these models also do not include the reformation and growth of SEI on Li metal due to the fracture of this layer upon dissolution and deposition of Li.

Among existing models that consider such complications (namely porosity) to some extend are comprehensive studies on graphite anode by Single et al. who predict the SEI thickness as well as porosity considering both inwards and outwards transport of the charge carries using an electrochemical model.[27] The authors demonstrate the dominance of specific laws unique to the SEI properties from electron transport-controlled to solvent-diffusion-controlled growth via the evolving porosity factor enabling the transition of the growth mechanism. The authors develop the model further to address the long-term growth behavior for cells stored at the different state of charge by considering all the plausible growth mechanism including electron tunneling and conduction, diffusion of electrolyte as well as neutral radicals such as Li interstitials, with the later confirmed to be the responsible parameter for longer time.

Additionally, Pinson et al. considered the collapse of the SEI and adopted their model to anodes which are subjected to expansion during lithiation, such as silicon nanoparticles.[21b] In such cases, the collapse of SEI induced by stress-build-up results in the continuous reformation and growth of new layer fragments. The authors analogously indicated that this results in a transformation from the parabolic law to linear regime confirmed experimentally on silicon anodes. Von Kolzenberg et al. who extended the model from Ref. [27c] for cycling conditions, similarly observe a transition from linear to square-root to linear corresponding to transition from reaction to diffusion to migration-limited growth mechanism.[28] The authors however suggested that the transition to the linear regime for the ultra-long time is inherent to the electrochemistry of SEI growth and not necessarily solely due to the cracks and reformation. On a rare attempt on Li metal, Thirumalraj et al. developed a Li-SEI model to investigate the determinants of Li nucleation and growth mechanism associated with SEI formation.[29] In the Li-SEI model three-dimensional diffusion-controlled growth process along with the simultaneous electrolyte decomposition upon the SEI collapse are taken into consideration. It is demonstrated that the electrolyte decomposition rate increases upon Li deposition and at higher overpotentials, mainly due to the partial breakdown of the SEI. Given the importance of this topic, both for understanding the nature of the SEI as well as for application, some origins of this detrimental phenomenon are detailed in the following.

## 3. Stability of the SEI on Li Metal

### 3.1. Breakdown Mechanism of the SEI on Li Metal

Even under optimal circumstances (non-porous and fully-intact SEI) transfer of the $Li^+$ to the SEI and through the SEI as well as across the SEI/electrolyte interface induced by the potential drop within the film is not the only possible charge transfer and transport pathway. Processes such as inward anion transfer promoted by the defects or electron transfer, occurring as a result of oxidation/reduction reactions at the SEI/electrolyte in combination with the essential electron conducting or semiconducting behavior of the SEI components, are other routes, shown in Figure 3aa. Additionally, complexing of cations at the SEI surface forming soluble species can proceed enhancing the transfer of $Li^+$ from the SEI to the electrolyte. In reality the electrode kinetics at the passivated state is indeed more complicated than these simplified processes. Such considerations of the charge transfer and transport impassive to the concentration of $Li^+$ ions in the solution as well as the morphology and composition of the SEI are far from the real systems. The charge transfer is complicated by the SEI layer formed between the metal electrode and the liquid electrolyte and hence dictated by the coupled electronic and ionic mobility in this layer. The passivation layer on Li is far from a homogenous and perfect structure showing defects at grain boundaries of oxides, disordered or amorphous regions, porosity and step edges among others, serving as vulnerable sites where damage can potentially strike. Thus, these defects constitute sites of greater reactivity, and accordingly the potential drop will be redistributed as shown in Figure 3bb resulting in an acceleration of the electrochemical reactions at these sites. This redistribution will disturb the homogeneity of the stripping/plating process. This is indeed investigated and discussed comprehensively in literature for plating as it is associated with the dendrite formation crucial to the battery

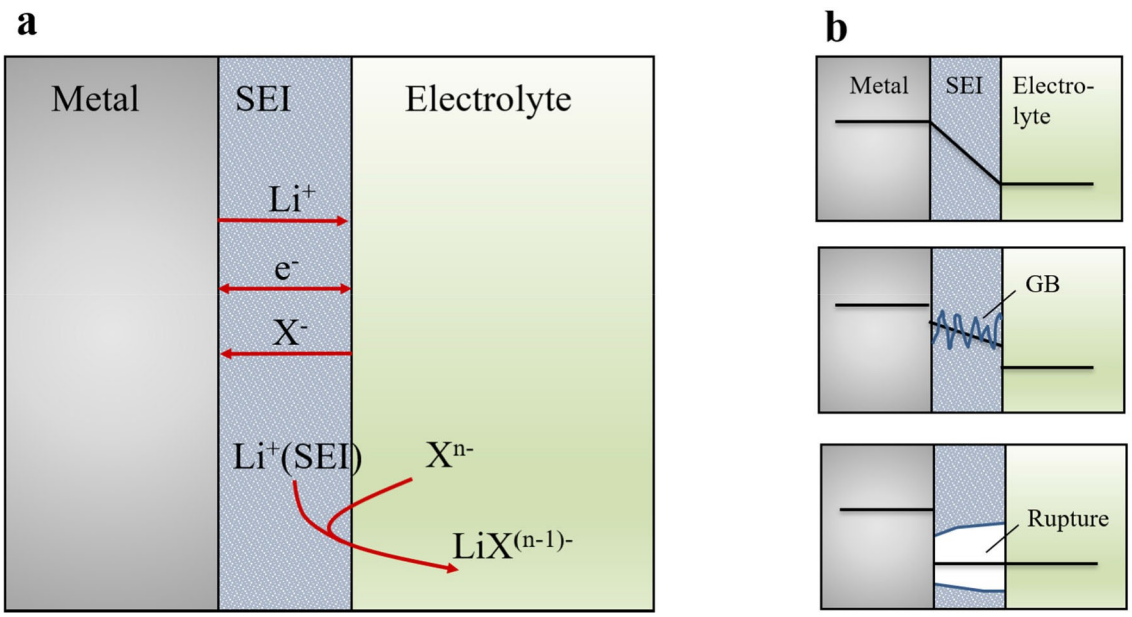


**Figure 3.** a) Few possible charge transport and transfer mechanisms in a non-porous SEI b) Redistribution of potential induced by grain boundary or porosity.[10,30]

safety during operation.[8e,31] Therefore, here we exemplarily discuss possible consequences of such a potential redistribution on the stripping process:[30]

(i) Local thinning and dissolution of the oxide layer: For the case of the greater potential drop at the SEI/electrolyte interface mentioned in the previous section, where the cations are bound by less extent to the oxide matrix, the $Li^+$ transfer from the SEI to the electrolyte will increase on account of a lower free activation enthalpy. The enhanced cation transfer triggered by the potential drop accelerates the localized dissolution of the passive layer resulting in local thinning of the SEI and variation of the potential profile, as shown schematically in Figure 4a. Taking into account the applied electrode potential, a larger gradient in potential develops at the SEI/el interface accelerating the electrochemical reactions. This ultimately results in depassivation in the less resistant areas where faster local dissolution is not compensated by superimposed film growth. However, this is probably very brief due to the self-healing effect of natural SEI at this point. Nevertheless, short-term pitting still occurs in the transient active state ahead of reformation. Temporary local breakdowns and pit formation are indeed very common and reported for Li stripping specifically at the early stages of cycling where the SEI is not sufficiently thick.[32] Another issue associated with this process, is the formation of so-called "dead-Li", where previously deposited Li may separate from the anode as the consequence of transient collapse of the SEI and remain electronically disconnected. In an interesting recent study Tzach Mukra et al. elucidate the capacity loss corresponding to the SEI repair process as well as formation of the dead lithium upon stripping for Li metal anodes in carbonate-based electrolytes.[33] The authors record a decrease in both $R_{SEI}$ and $L_{SEI}$ with cycling explained by the increase in surface roughness due to the formation of porous Li.

(ii) Metal voiding: In the case that the larger potential drop is indeed located at the metal/SEI interface a faster local reaction would be triggered, Figure 4b. The localized repressed regions in the metal surface at the metal/SEI interface develops for the ionically conductive SEI, where the accelerated transport of the new cations through reactive sites of the SEI layer is associated with their enhanced transfer to the electrolyte. Metal vacancies ($V_{Li}$) begin to accumulate at the metal surface and generate interfacial voids. The void accretion at this interface when not counterbalanced by the outwards diffusion, leads to local stress build-up and eventual depassivation, observed experimentally for Li metal anode.[34] Shi et al. interestingly demonstrate the fast accumulation of voids at the interface of Li/SEI under high current density, causing the ultimate collapse of the SEI layer and the initiation of further pitting.

(iii) Particle deposition and growth at the metal/SEI interface followed by rupture of the SEI: Another ion transport induced complication occurs when anions penetrate the SEI layer via defective sites or explained by point-defects and diffuse to the metal/SEI interface or inside the SEI with the newly formed cations, forming Li compounds (e.g., $LiO_2$, LiF, $Li_2S$, etc.) at this inner interface or in the SEI.[10,30] This counteracting process to the void formation accompanied with stress generation in the SEI as well, leading to the local breakdown, see Figure 4c.

Given this discussion and theses examples, any factor that interferes with the required charge transfer at the SEI/electrolyte and metal/SEI interface and diffusion through the SEI layer

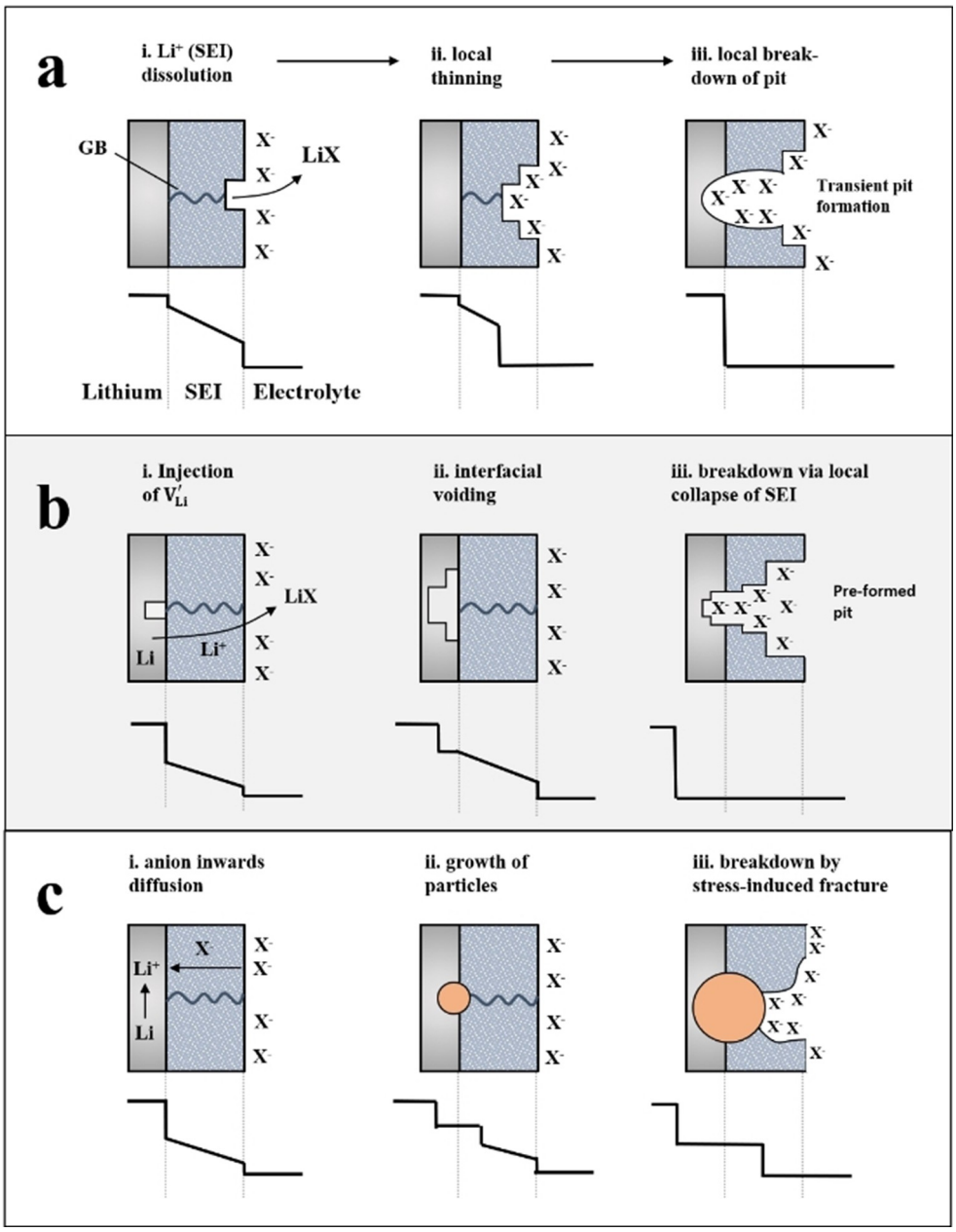


**Figure 4.** Enhanced dissolution at defect sites available in the SEI and consequential breakdown mechanism upon stripping as the result of redistribution of potential: a) local thinning b) metal voiding c) deposition at the metal/SEI interface. Adapted from Ref. [30] with permission Copyright (2008) Elsevier.

will inevitably generate increased local dissolution or deposition and consequently initiate the collapse of the SEI. In the following, a number of critical parameters causing inhomogeneous deposition and dissolution of the metal and the corresponding instability of the SEI layer will be addressed.

### 3.2. Electrolyte Properties Crucial to the Stability of the SEI

#### *3.2.1. Chemical Properties: Composition and Morphology of the SEI*

The electrolyte components including solvent, salt and the additives define the morphology and composition of the formed SEI on Li metal.[35] Considering the break-away mechanism explained in the previous section activation energy and concentration of the defects, migration and diffusion barrier of cation interstitials and vacancies, anion diffusion are factors of substantial significance to the smooth charge transfer and transport.

The intrinsic SEI of Li metal in contact with liquid electrolyte consists of a variety of different components depending on the composition of the electrolyte with the various species strongly influencing transport properties and stability to different degrees, as outlined in the following for important examples. A $Li_3N$-based SEI, which has a lower interfacial resistance, is among one of the favorable protection layers.[36] Nitrogen comprising salts such as lithium 2-trifluoromethyl-4,5-dicyanoimidazole (LiTDI) and $LiNO_3$ as additive are of instances forming $Li_3N$-based SEI, the latter which is commonly applied in laboratory Li-sulfur cells.[13,37] The ionic conductivity of $\alpha$-$Li_3N$ and $\beta$-$Li_3N$ at room temperature is about $10^{-4}\,S\,cm^{-1}$.[38] The activation energies for Li ion diffusion in $\alpha$-$Li_3N$ and $\beta$-$Li_3N$ are reported to be 0.427 eV and 0.448 eV, respectively, predominately caused by the defect formation energy given a relatively lower migration energy barrier of 0.007 eV( $\alpha$-$Li_3N$) and 0.038 eV ($\beta$-$Li_3N$).[39] The LiF enriched SEI is yet another advantageous composition, which has been induced using the LiF itself as an additive or various other fluorine containing additives such as fluoroethylene carbonate (FEC), improving stability of the SEI and suppressing dendritic Li growth.[40] The LiF with cation vacancies as the dominant carriers shows relatively high diffusion barrier of at least 0.7 eV accompanied by suppressed electronic conductivity.[41] The ionic conductivity of $10^{-31}\,S\,cm^{-1}$ at the anode potential is calculated for LiF.[42] The surface Li adatom diffusion barrier on the other hand has been reported to be sufficiently low, which is the main reason deployed to elucidate the superior performance of the LiF-based SEI.[43] In contrary for $Li_2CO_3$, reported in the SEI layer formed in the presence of typically employed electrolytes in Li-based cell chemistries (ether and carbonates), the main defects in contact with negative electrode are Li ion interstitials with its charge balanced by electrons, resulting in relatively high ionic conductivity ($\sim 10^{-11}$–$10^{-8}\,S\,cm^{-1}$) while containing a considerable electron concentration explaining the poor performance as SEI compound.[44] The defect chemistry of the $Li_2O$ as an inevitable component of SEI has been studied in details.[45] The ionic conductivity of around $10^{-12}\,S\,cm^{-1}$ and the electronic conductivity of less than or equal to $10^{-14}\,S\,cm^{-1}$ under oxidizing conditions are reported. Such low electronic conductivity explains the implication of the dry room and the preference of the $Li_2O$ to LiOH and $Li_2CO_3$. $Li_2O$ is experimentally detected quite often in the inner layer of the SEI corroborating the DFT calculations.[46]

Further experimental work on the charge carrier chemistry of the thin film of these compounds at anode potential as a study model would be of great essence for understanding the performance and the design of the artificial SEI.

The heterogeneity of the SEI and interfaces between these inorganic compounds should be considered as a distinguishing factor. Among the studied grain boundaries, the faster Li diffusion rate is reported for the LiF/$Li_2O$ in comparison to the LiF/LiF and $Li_2O$/$Li_2O$, explained by the favorable structure of Li multiatom coordination inside the grain boundary resulting in the preferred multiatom hopping mechanism.[47] It is experimentally illustrated and discussed that the LiF and $Li_2CO_3$ interface is accompanied with the redistribution of the Li ion resulting in enhancement of the charge carrier ( $V'_{Li}$ in LiF and $Li_{Li}$ in $Li_2CO_3$) suppressing the electronic conductivity analogous to the LiF/$TiO_2$ interface.[48] Interestingly, the doped LiF at the anode potential results in an increase in the cation vacancy concentration enhancing the ionic conductivity, while in the case of the $Li_2O$ the doping is suggested to be relatively ineffective, due to the low solubility of dopants.[42,45, 49] This observed enhancement in ionic conductivity via doping in LiF could be another explanation of the superior performance of the LiF enriched SEI despite the higher diffusion barrier values. Therefore, any structural configuration increasing the ionic conductivity and lowering the diffusion barrier as well as suppressing the electronic conductivity would be of imperative importance to the stability of the SEI layer.

The $Li^+$ diffusion in the SEI ($D^{SEI}_{Li+} \sim 10^{-12}\,cm^2\,s^{-1}$) and resistivity (in the order of $10^2$–$10^3\,\Omega\,cm^2$) values reported for the practical SEI on Li metal in contact with the liquid electrolyte are substantially at variance from that of these inorganic compounds, indicating the SEI cannot be solely comprised of these inorganic species.[15b] Indeed there has been many efforts since the 1980's to understand the morphology and chemical structure of the SEI.[50] The mosaic structure introduced by Peled and the multilayer one suggested by Aurbach have been already indicated in Figure 2. The technological progression in electron microscopy methods such as the ability to study surfaces and interfaces under cryogenic conditions in the recent years has shed light on the structure and morphology of the SEI on Li metal.[24,26,51] Both mentioned morphologies regulated by the electrolyte have been confirmed. Among these studies, Hou et al. reported bilayer structure of the SEI films with an inner inorganic layer and outer organic one using *operando* Mass-Sensitive Scanning Transmission Electron Microscopy.[52] The SEI film appears to undergo a transition from an initial porous and non-uniform inorganic/organic bilayer to a more uniform film comprised of a solid inorganic layer/porous organic layer, due to diffusion of the radical species through the observed voids. This results in the transition of lithiation from the short-range to the long-range diffusion upon charge. In contrast to this observation, the mosaic configuration in EC/DEC electrolyte as well as the multilayer structure comprised of amorphous organic inner layer and inorganic outer layer, see Figure 2e, in FEC-based electrolyte has been confirmed using cryogenic electron microscopy by Li et al.[26] The multilayer structure has been suggested to facilitate a more uniform dissolution of Li and superior performance. The highly feasible consequence of mosaic morphology is that the structural heterogeneity including grain boundaries, compositional and morphological gradients triggers the preferential deposition and dissolution of the Li ion. The occurrence of the mosaic or multilayer structure is attributed to the reduction potential of the components in electrolyte and therefore system dependent. Another plausible explanation for the superior behavior of the additive containing electrolytes such as $LiNO_3$ and LiF with the low reduction potential is the accelerated formation of LiF and $Li_3N$ resulting in the multilayer structure with the ability of keeping the

structure in the case of the SEI breakdown due to the fast-self-healing properties of these electrolytes.

Additionally, it is disputed that the picture is more complicated than the case that the dominant factor in the regulation of charge transport and transfer, stems solely from the defect chemistry of inorganic compounds. The presence of elastomer and polymer component specifically in FEC-based electrolytes has shown to play a crucial role as well. Li et al. demonstrated that LiF is not effectively present in the compact SEI and accordingly not playing a substantial role to the transport process of $Li^+$.[24] The authors suggest the rapid defluorination at the anode and subsequent polymerization induced by FEC additives is indeed the responsible factor for enhancement in SEI stability and performance. Interestingly, He et al. have demonstrated that the formed in-situ LiF accompanied with an elastomeric outer layer with the ability of self-healing is more stable and effective in suppressing the dendritic Li deposition than the ex-situ formed homogenous single layer LiF.[53] Recent NMR studies on the Li-SEI interface corroborates the existence of polymeric species and LiF in the SEI in contact with electrolytes containing FEC as additives.[54]

Additionally, recent studies have reported the formation of a thin (~10 nm) homogeneous, amorphous and monolithic SEI layer on Li metal exposed to the newly designed electrolyte composition based on a fluorinated orthoformate solvent.[55] This SEI layer is rich in inorganic species suppressing Li loss and volumetric expansion.

These aforementioned studies collectively highlight the consequential stability of SEI under the presence of amorphous phases in deeper layers on Li metal.

### 3.2.2. Transport Properties of Electrolyte and Current Density

Conventional salt containing liquid electrolytes exhibit both anion and cation conductivity. In such electrolyte systems with cationic and anionic mobile species, under polarization, where the anion flux is not supported by the blocking electrode, the mobile anions migrate and accumulate at the positive electrode surface (the anionic flux eventually disappears at the steady-state conditions), leading to the formation of a concentration gradient. Here the cation concentration gradient is forced by electroneutrality.[56] This concentration gradient restricts the charge/discharge rate and establishes a concentration polarization that sets limits on the operating voltage of the cell, thereby constraining the power and energy density parameters.

The Li transference number is a measure indicating the ratio of cation conductivity ($\sigma_+$) to the overal conductivity [Eq. (14)]:

$$t_+ = \frac{\sigma_+}{\sigma_+ + \sigma_-} \tag{14}$$

The non-unity value of the $Li^+$ transfer number ($t_+$) leads to the mentioned concentration polarization, which could expand to the whole electrolyte. Transference number is a critical issue for Li metal batteries employed at higher current densities. However, the development of organic electrolytes with high transference number as well as conductivity remains difficult as the conductivity is compromised in systems with demobilized anion.

The concentration gradient induced by galvanostatic polarization in the Li/Li symmetrical cell with reduced electrode spacing was investigated by Brissot et al. [Eq. (15)]:[8b]

$$\frac{\partial c}{\partial x}(x) = \frac{J\mu_+}{eD(\mu_+ + \mu_-)} \tag{15}$$

where $J$ is the effective current density, $D$ the ambipolar diffusion coefficient, $e$ the electronic charge, $\mu_-$ and $\mu_+$ are the anion and cation mobilities. At lower current densities, the ionic concentration develops from the initial ($c_o$) to a steady state values (a constant concentration gradient) where the concentration linearly increases from $c_a = c_o - \Delta c$ at the negative electrode to $c_c = c_o + \Delta c$ at the positive electrode ($dc/dx < 2c_o/L$) shown in Figure 5a. In contrast, polarizing the cell with higher current density causes the ion concentrations to approach zero near the negative electrode ($dc/dx > 2c_o/L$). The authors observed that the dendrite formation is promoted upon cycling at higher current densities. It is also imaginable that the depletion in concentration of the $Li^+$ at the vicinity of SEI layer

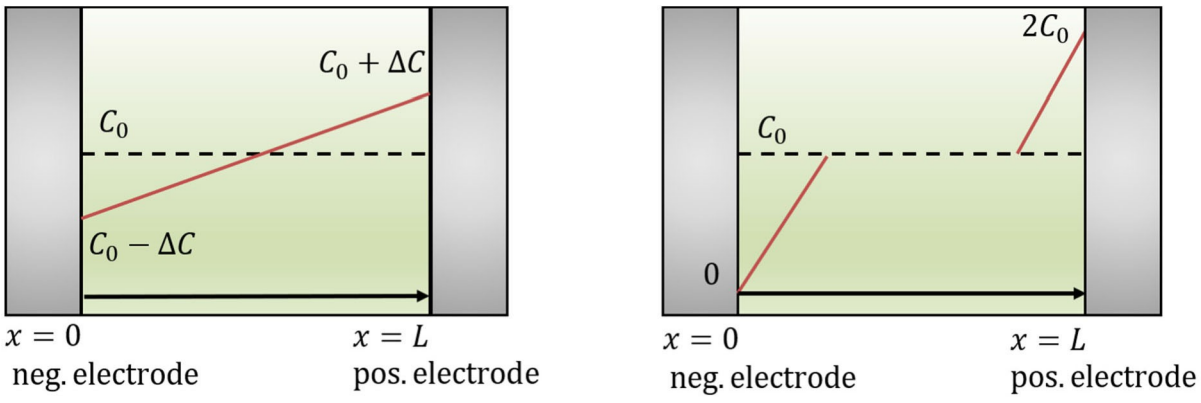


**Figure 5.** Concentration gradient buildup a) at low current density b) high current density.[8b]

enhances the dissolution of the $Li^{+}{}_{SEI/electrolyte}$ leading to the formation of voids and eventually depassivation, detrimental to cell performance.

Integrating equation 15, the current density could be rewritten as [Eq. (16)]:[57]

$$J^{*} = \frac{2ec_0D}{t_{-}L} \tag{16}$$

where $J^{*}$ is the limiting current density, $c_0$ is the initial $Li^{+}$ concentration, $L$ is the thickness of diffusion layer, $t_{-}$ is the anion transference number given by $\frac{\mu_{-}}{\mu_{-}+\mu_{Li^{+}}} = 1 - t_{+}$. Therefore, enhancement in $c_0$ and $t_{+}$ increases the critical current density which hinders dendrite formation, demanding the design of electrolyte systems with increased $t_{+}$. Single-ion-conductor solid electrolytes as well as solid-liquid composite electrolytes with enhanced transference number are commonly employed systems addressing this issue.[58] Alternatively, to lower the diffusion pathway and diminish the concentration polarization at the interface during electroplating, stirring and high-frequency pulse currents are employed to enhance the convection rates in electrolyte.[59] Similarly, the periodic reverse pulse is reported to effectively boost the $Li^{+}$ diffusion rate improving Li deposit morphology and Li cycling efficiency. Here it should be emphasized that the current density is not just matter of importance considering polarization build-up, but also in terms of morphology of the deposited Li and formation of the dendritic or mossy structures.[8e,60] Furthermore, the effect of current density during formation phase on the morphology and composition of the SEI itself is of crucial significance and needs to be investigated as well. On graphite it is indicated that the SEI formed at lower current densities is comprised of more organic and less inorganic Li compositions deposited uniformly on the surface of the graphite anode as compared with higher formation current density.[61]

## 4. Implications of Practical Cell and Cycling Conditions on SEI Studies

The influence of current density on the evolution of the SEI layer and its stability upon cycling is an important example of how the demands from application dictate the requirements to the SEI properties. It is clear that a thorough understanding of the role of the various SEI components and of the SEI structure in guiding the macroscopic cell performance is an essential prerequisite for the development of protection strategies for Li metal. Still, we want to emphasize that the implications of practical cell and cycling conditions need to be considered already at an early stage to fully leverage this knowledge for a successful cell design. More specifically, moving from laboratory cells suitable for fundamental studies to more practically relevant cell designs (e.g., pouch cells) with competitive energy density, there are several factors that can drastically change the outcome of such investigations. Of important differences are the cell size and the corresponding total current, the ratio of electrolyte to active material, the amount of Li excess, pressure conditions, cross-talk between anode and cathode as well as the cathode loading, a factor determining the amount of cycled Li per cycle. In light of this, the transition of the results obtained at the coin cell level into functional and practical pouch cells remains challenging regardless of employment of natural or in/ex situ artificial SEI. The need for a better alignment of early-stage studies and requirements imposed by application has been emphasized by several recent contributions.[62]

In principle, the underlying chemistry of the intrinsic SEI layer should not be affected substantially by these changes, yet, the stability of the SEI is more challenged as stress-induced damage by the harsh conditions becomes more severe. Accordingly, all the above factors can cause seemingly promising anode protection strategies developed in laboratory cells to fail under more realistic conditions. In addition, in many such cases, cell failure is masked by plentiful electrolyte and Li reservoir.[63] However, only a few studies have looked at how the SEI characteristics as well as the morphology evolution of Li during stripping and plating evolve under practical conditions or even in larger-format pouch cells and what this entails for the design of an efficient SEI strategy.[63–64]

An insightful study in this respect is the work published by Shi et al. who studied how pouch cells with thin Li foil (50 μm, 10 mAh $cm^{-2}$) fail as function of current density, cycling capacity and Li utilization (determined by cathode loading and the Li thickness).[65] Two important factors which can significantly alter the outcome of studies on SEI properties and metal protection are stressed therein: i) the effect of cycling capacity as often neglected cycling parameter and ii) cell failure by dead Li formation which is often masked by excessive availability of Li in thick foils. In applications with high energy density requirements, areal capacity will progress towards 4 mAh $cm^{-2}$ or larger and might well exceed 6 mAh $cm^{-2}$ for next-generation batteries (e.g., for Li–S with practical sulfur loading $>5$ $mg_S$ $cm^{-2}$).[66] In such cases with very high capacity cycling, short-circuit occurrence due to dendrite growth during plating is suggested to be the main failure mode, already at moderate current densities.[65] Due to the enormous amount of Li which is cycled, the accompanying volume change makes flexibility of the SEI layer, as obtained for example by polymerization in FEC-based electrolytes (see above), an essential characteristic in this case. On the other hand, at low capacity cycling ($<$ 2 mAh $cm^{-2}$ and also higher, depending on current density) in liquid electrolyte cells, the failure mode commonly stems from pulverization of Li due to gradual consumption of bulk Li and accumulation of dead Li, as also stressed by Fang et al.[62b] Here, the current density has a strong influence on cycle life. At low current density, the driving force is not high enough in relation to the migration resistance to activate a significant amount of bulk Li which is shielded by a thick SEI layer. The Li surface remains relatively flat and dense. However, at higher rates, porous Li is generated much faster and the degradation layer comprised of porous and electronically isolated Li is expanded deep into the bulk.[65] A similar observation for the effect of plating current density on Li corrosion and cycled capacity (up

to moderate values) is reported by Jiao et al. The study demonstrated a substantially increased degradation layer in case of both high current or capacity.[67] This is accompanied by a concurrent change in the composition of the SEI which unfortunately is not elaborately discussed. Since there is a large reservoir of bulk Li when thick foils are used as it is common in coin-cell studies, cell failure can be drastically shifted to high cycle number although at practical Li thickness failure could happen already after a handful of cycles.

The morphological changes and structural evolution of Li which challenge the stability of the SEI and contribute to dead Li generation can be mitigated to a certain degree by the application of a defined external pressure in the normally pressure-free pouch cells.[68] The significance of this has for example been demonstrated by Niu et al.[66a] Accordingly, the external pressure facilitates a more uniform and compact plating behavior which is beneficial for SEI stability and helps in the suppression of dendrite formation.[69] An additional effect of the more compact Li morphology is the lower fresh surface area which if not effectively shielded against electrolyte will entail additional SEI formation and capacity loss. At the same time contact between Li particles inside the porous structures created by prolonged cycling is improved, thereby, slowing down the generation of dead Li fractions.[66a] While all these factors can decelerate degradation, the magnitude of the underlying mechanisms, *i.e.* uniformity of stripping and plating as well as protection of Li against electrolyte, are all determined by the effectiveness of the SEI. The pressure in laboratory cells which is often not well defined and deviates between different cell types might reduce the requirements on stability and effectiveness of the artificial SEI layer and make their failure not as drastically visible as would be the case in a pressure-free or -reduced system. It is therefore important that studies on the design of SEI solutions resemble the pressure conditions encountered in application or at least take possible discrepancies into account.

Even when using practical conditions and synchronizing the parameters between these types of studies, additional complexity arises due to the non-uniform distribution of the macroscopic current density when scaling up Li metal cells. This can in turn induce gradients in local state-of-charge and temperature inside the cell. This effect has been shown to be critical in Li-ion batteries leading to pronounced non-uniform degradation over cycle life which strongly compromises longevity.[70] This will play an even more pronounced role for Li metal cells, where already small defects or protrusions accelerate degradation over cycle life. Accordingly, inhomogeneous Li stripping/plating behavior under SEI with non-ideal transport properties is therefore detrimental.[66a] Due to the voltage drop along the electrode length, the local current density and therefore stress is highest close to the tabs in a pouch cell which can initiate a severe and continuing amplification of degradation in this region. This will inevitably reduce cycle life according to the above discussed stress-induced deterioration of the SEI layer. As a result of the non-uniform current density distribution and current peaks at critical positions, this effect can already proceed at current densities which were shown to be safe in coin-cell tests. Even more than in a Li-ion cell, it is therefore crucial to ensure homogeneous behavior along the electrode stack or at least keep this situation in mind and be able to understand the behavior. So far, although of high relevance for upscaling, this topic has not been studied for Li metal pouch cells.

## 5. Conclusions

This article provides an overview of the relevant and applicable studies on the formation and growth mechanism of SEI on Li metal during storage as well as the cycling conditions. Emphasis is placed on how the morphology and composition of the SEI potentially influences the charge transport and transfer mechanism, resulting in varying growth behavior and overall stability. A crucial insight is that the morphology and composition of the SEI on Li metal, the SEI growth behavior, the determining failure mechanism and consequential capacity loss are highly case-dependent due to influential parameters such as electrolyte and current density, among others. It is therefore proposed to avoid generalization and to choose the style of the case- study for further reports on Li metal. Additionally, models considering the stress-induced fracture, dead-lithium formation as well as various conduction pathways corresponding to the SEI composition and morphologies needs to be further develop and modified for the SEI on Li metal anode.

Concerning the application, albeit strategies such as the application of external pressure and the use of three-dimensional hosts have been shown to mitigate challenges associated with Li metal, the nature of the intrinsic SEI remains unchanged. Accordingly, its stability and ability to protect the metal surface are still the bottleneck and key feature for enabling the commercialization of Li metal cells. Importantly, this holds true also when solid electrolytes are employed: only when a stable interface with the desired properties is formed between Li and the solid electrolyte, an efficient Li metal cell can become reality.

## *Acknowledgements*

*Open access funding enabled and organized by Projekt DEAL.*

## *Conflict of Interest*

The authors declare no conflict of interest.

**Keywords:** lithium metal · solid-electrolyte interphase · liquid electrolyte · batteries · energy storage

[1] M. Armand, P. Axmann, D. Bresser, M. Copley, K. Edström, C. Ekberg, D. Guyomard, B. Lestriez, P. Novák, M. Petranikova, W. Porcher, S.

Trabesinger, M. Wohlfahrt-Mehrens, H. Zhang, *J. Power Sources* **2020**, *479*, 228708.
[2] T. Placke, R. Kloepsch, S. Dühnen, M. Winter, *J. Solid State Electrochem.* **2017**, *21*, 1939–1964.
[3] D. Lin, Y. Liu, Y. Cui, *Nat. Nanotechnol.* **2017**, *12*, 194–206.
[4] a) A. Varzi, K. Thanner, R. Scipioni, D. Di Lecce, J. Hassoun, S. Dörfler, H. Altheus, S. Kaskel, C. Prehal, S. A. Freunberger, *J. Power Sources* **2020**, *480*, 228803; b) R. Wang, W. Cui, F. Chu, F. Wu, *J. Energy Chem.* **2020**, *48*, 145–159; c) Y. Zhang, T.-T. Zuo, J. Popovic, K. Lim, Y.-X. Yin, J. Maier, Y.-G. Guo, *Mater. Today* **2020**, *33*, 56–74; d) J. Zheng, M. S. Kim, Z. Tu, S. Choudhury, T. Tang, L. A. Archer, *Chem. Soc. Rev.* **2020**, *49*, 2701–2750.
[5] a) A. M. Andersson, K. Edström, *J. Electrochem. Soc.* **2001**, *148*, A1100; b) K. Edström, M. Herstedt, D. P. Abraham, *J. Power Sources* **2006**, *153*, 380–384; c) J. Vetter, P. Novák, M. R. Wagner, C. Veit, K. C. Möller, J. O. Besenhard, M. Winter, M. Wohlfahrt-Mehrens, C. Vogler, A. Hammouche, *J. Power Sources* **2005**, *147*, 269–281.
[6] P. Keil, S. F. Schuster, J. Wilhelm, J. Travi, A. Hauser, R. C. Karl, A. Jossen, *J. Electrochem. Soc.* **2016**, *163*, A1872-A1880.
[7] X.-B. Cheng, R. Zhang, C.-Z. Zhao, Q. Zhang, *Chem. Rev.* **2017**, *117*, 10403–10473.
[8] a) R. Akolkar, *J. Power Sources* **2013**, *232*, 23–28; b) C. Brissot, M. Rosso, J. N. Chazalviel, S. Lascaud, *J. Power Sources* **1999**, *81–82*, 925–929; c) J. N. Chazalviel, *Phys. Rev. A* **1990**, *42*, 7355–7367; d) M. l. Dollé, L. Sannier, B. Beaudoin, M. Trentin, J.-M. Tarascon, *ESL* **2002**, *5*, A286; e) G. Liu, W. Lu, *J. Electrochem. Soc.* **2017**, *164*, A1826-A1833; f) K. Nishikawa, T. Mori, T. Nishida, Y. Fukunaka, M. Rosso, *J. Electroanal. Chem.* **2011**, *661*, 84–89; g) M. N. Parekh, C. D. Rahn, L. A. Archer, *J. Power Sources* **2020**, *452*, 227760.
[9] a) X.-B. Cheng, R. Zhang, C.-Z. Zhao, F. Wei, J.-G. Zhang, Q. Zhang, *Adv. Sci.* **2016**, *3*, 1500213; b) Z. Tu, S. Choudhury, M. J. Zachman, S. Wei, K. Zhang, L. F. Kourkoutis, L. A. Archer, *Joule* **2017**, *1*, 394–406; c) Z. Yu, Y. Cui, Z. Bao, *Cell Reports Physical Science* **2020**, *1*, 100119.
[10] P. Marcus, *Corrosion Mechanisms in Theory and Practice*, CRC Press, **2011**.
[11] M.-H. Ryou, Y. M. Lee, Y. Lee, M. Winter, P. Bieker, *Adv. Funct. Mater.* **2015**, *25*, 834–841.
[12] N. B. Hannay, *Treatise on Solid State Chemistry: Reactivity of solids. Vol. 4*, Plenum, **1976**.
[13] M. Nojabaee, K. Küster, U. Starke, J. Popovic, J. Maier, *Small* **2020**, *16*, 2000756.
[14] N. Cabrera, N. F. Mott, *Rep. Prog. Phys.* **1949**, *12*, 163–184.
[15] a) E. Peled, *J. Electrochem. Soc.* **1979**, *126*, 2047–2051; b) A. Kushima, K. P. So, C. Su, P. Bai, N. Kuriyama, T. Maebashi, Y. Fujiwara, M. Z. Bazant, J. Li, *Nano Energy* **2017**, *32*, 271–279.
[16] S. Shiraishi, K. Kanamura, Z. I. Takehara, *J. Appl. Electrochem.* **1999**, *29*, 867–879.
[17] C. Wagner, *J. Electrochem. Soc.* **1956**, 57.
[18] H. Schmalzried, *Solid State Reactions*, VCH: Weinheim, Germany **1981**, p. 170–180.
[19] S. Wenzel, S. J. Sedlmaier, C. Dietrich, W. G. Zeier, J. Janek, *Solid State Ionics* **2018**, *318*, 102–112.
[20] D. Aurbach, *J. Power Sources* **2000**, *89*, 206–218.
[21] a) M. Nie, D. P. Abraham, Y. Chen, A. Bose, B. L. Lucht, *J. Phys. Chem. C* **2013**, *117*, 13403–13412; b) M. B. Pinson, M. Z. Bazant, *J. Electrochem. Soc.* **2012**, *160*, A243-A250; c) H. J. Ploehn, P. Ramadass, R. E. White, *J. Electrochem. Soc.* **2004**, *151*, A456; d) F. Röder, R. D. Braatz, U. Krewer in *Multi-Scale Modeling of Solid Electrolyte Interface Formation in Lithium-Ion Batteries, Vol. 38* Eds.: Z. Kravanja, M. Bogataj), Elsevier, **2016**, pp. 157–162; e) M. Steinhauer, M. Stich, M. Kurniawan, B.-K. Seidlhofer, M. Trapp, A. Bund, N. Wagner, K. A. Friedrich, *ACS Appl. Mater. Interfaces.* **2017**, *9*, 35794–35801; f) M. Tang, J. Newman, *J. Electrochem. Soc.* **2011**, *158*, A530.
[22] J. Christensen, J. Newman, *J. Electrochem. Soc.* **2004**, *151*, A1977.
[23] S. Das, P. M. Attia, W. C. Chueh, M. Z. Bazant, *J. Electrochem. Soc.* **2019**, *166*, E107-E118.
[24] Y. Li, Y. Li, A. Pei, K. Yan, Y. Sun, C.-L. Wu, L.-M. Joubert, R. Chin, A. L. Koh, Y. Yu, J. Perrino, B. Butz, S. Chu, Y. Cui, *Science* **2017**, *358*, 506–510.
[25] M. Safari, M. Morcrette, A. Teyssot, C. Delacourt, *J. Electrochem. Soc.* **2009**, *156*, A145.
[26] Y. Li, W. Huang, Y. Li, A. Pei, D. T. Boyle, Y. Cui, *Joule* **2018**, *2*, 2167–2177.
[27] a) F. Single, B. Horstmann, A. Latz, *Phys. Chem. Chem. Phys.* **2016**, *18*, 17810–17814; b) F. Single, B. Horstmann, A. Latz, *J. Electrochem. Soc.* **2017**, *164*, E3132-E3145; c) F. Single, A. Latz, B. Horstmann, *ChemSusChem* **2018**, *11*, 1950–1955.
[28] L. von Kolzenberg, A. Latz, B. Horstmann, *ChemSusChem* **2020**, *13*, 3901–3910.
[29] B. Thirumalraj, T. T. Hagos, C.-J. Huang, M. A. Teshager, J.-H. Cheng, W.-N. Su, B.-J. Hwang, *J. Am. Chem. Soc.* **2019**, *141*, 18612–18623.
[30] P. Marcus, V. Maurice, H. H. Strehblow, *Corros. Sci.* **2008**, *50*, 2698–2704.
[31] X. Zhang, A. Wang, X. Liu, J. Luo, *Acc. Chem. Res.* **2019**, *52*, 3223–3232.
[32] H. Liu, X.-B. Cheng, R. Xu, X.-Q. Zhang, C. Yan, J.-Q. Huang, Q. Zhang, *Adv. Energy Mater.* **2019**, *9*, 1902254.
[33] T. Mukra, E. Peled, *J. Electrochem. Soc.* **2020**, *167*, 100520.
[34] a) J. Kasemchainan, S. Zekoll, D. Spencer Jolly, Z. Ning, G. O. Hartley, J. Marrow, P. G. Bruce, *Nat. Mater.* **2019**, *18*, 1105–1111; b) F. Shi, A. Pei, D. T. Boyle, J. Xie, X. Yu, X. Zhang, Y. Cui, *PNAS* **2018**, *115*, 8529–8534.
[35] a) D. Aurbach, I. Weissman, A. Zaban, O. Chusid, *Electrochim. Acta* **1994**, *39*, 51–71; b) G. Bieker, M. Winter, P. Bieker, *Phys. Chem. Chem. Phys.* **2015**, *17*, 8670–8679; c) S. Jurng, Z. L. Brown, J. Kim, B. L. Lucht, *Energy Environ. Sci.* **2018**, *11*, 2600–2608; d) E. Markevich, G. Salitra, F. Chesneau, M. Schmidt, D. Aurbach, *ACS Energy Lett.* **2017**, *2*, 1321–1326; e) Q. Shi, Y. Zhong, M. Wu, H. Wang, H. Wang, *PNAS* **2018**, *115*, 5676–5680.
[36] a) G. Ma, Z. Wen, M. Wu, C. Shen, Q. Wang, J. Jin, X. Wu, *Chem. Commun.* **2014**, *50*, 14209–14212; b) K. Park, J. B. Goodenough, *Adv. Energy Mater.* **2017**, *7*, 1700732.
[37] a) C. Xu, S. Renault, M. Ebadi, Z. Wang, E. Björklund, D. Guyomard, D. Brandell, K. Edström, T. Gustafsson, *Chem. Mater.* **2017**, *29*, 2254–2263; b) A. Rosenman, R. Elazari, G. Salitra, E. Markevich, D. Aurbach, A. Garsuch, *J. Electrochem. Soc.* **2015**, *162*, A470-A473.
[38] B. A. Boukamp, R. A. Huggins, *Mater. Res. Bull.* **1978**, *13*, 23–32.
[39] W. Li, G. Wu, C. M. Araújo, R. H. Scheicher, A. Blomqvist, R. Ahuja, Z. Xiong, Y. Feng, P. Chen, *Energy Environ. Sci.* **2010**, *3*, 1524–1530.
[40] a) S. Choudhury, L. A. Archer, *Adv. Electron. Mater.* **2016**, *2*, 1500246; b) D. Lin, Y. Liu, W. Chen, G. Zhou, K. Liu, B. Dunn, Y. Cui, *Nano Lett.* **2017**, *17*, 3731–3737; c) X.-Q. Zhang, X. Chen, R. Xu, X.-B. Cheng, H.-J. Peng, R. Zhang, J.-Q. Huang, Q. Zhang, *Angew. Chem. Int. Ed.* **2017**, *56*, 14207–14211; d) Y. Zhang, D. Krishnamurthy, V. Viswanathan, *J. Electrochem. Soc.* **2020**, *167*, 070554; e) J. Zhao, L. Liao, F. Shi, T. Lei, G. Chen, A. Pei, J. Sun, K. Yan, G. Zhou, J. Xie, C. Liu, Y. Li, Z. Liang, Z. Bao, Y. Cui, *J. Am. Chem. Soc.* **2017**, *139*, 11550–11558.
[41] a) Y. C. Chen, C. Y. Ouyang, L. J. Song, Z. L. Sun, *J. Phys. Chem. C* **2011**, *115*, 7044–7049; b) I. Kishida, Y. Koyama, A. Kuwabara, T. Yamamoto, F. Oba, I. Tanaka, *J. Phys. Chem. B* **2006**, *110*, 8258–8262; c) H. Yildirim, A. Kinaci, M. K. Y. Chan, J. P. Greeley, *ACS Appl. Mater. Interfaces* **2015**, *7*, 18985–18996.
[42] J. Pan, Y.-T. Cheng, Y. Qi, *Phys. Rev. B* **2015**, *91*, 134116.
[43] Y. Ozhabes, D. Gunceler, T. A. Arias, *J. Mater. Sci.* **2015**.
[44] S. Shi, Y. Qi, H. Li, L. G. Hector, *J. Phys. Chem. C* **2013**, *117*, 8579–8593.
[45] S. Lorger, R. Usiskin, J. Maier, *J. Electrochem. Soc.* **2019**, *166*, A2215-A2220.
[46] K. Leung, F. Soto, K. Hankins, P. B. Balbuena, K. L. Harrison, *J. Phys. Chem. C* **2016**, *120*, 6302–6313.
[47] A. Ramasubramanian, V. Yurkiv, T. Foroozan, M. Ragone, R. Shahbazian-Yassar, F. Mashayek, *J. Phys. Chem. C* **2019**, *123*, 10237–10245.
[48] a) J. Pan, Q. Zhang, X. Xiao, Y.-T. Cheng, Y. Qi, *ACS Appl. Mater. Interfaces* **2016**, *8*, 5687–5693; b) C. Li, L. Gu, X. Guo, D. Samuelis, K. Tang, J. Maier, *Nano Lett.* **2012**, *12*, 1241–1246.
[49] C. Li, L. Gu, J. Maier, *Adv. Funct. Mater.* **2012**, *22*, 1145–1149.
[50] E. Peled, S. Menkin, *J. Electrochem. Soc.* **2017**, *164*, A1703-A1719.
[51] M. J. Zachman, Z. Tu, S. Choudhury, L. A. Archer, L. F. Kourkoutis, *Nature* **2018**, *560*, 345–349.
[52] C. Hou, J. Han, P. Liu, C. Yang, G. Huang, T. Fujita, A. Hirata, M. Chen, *Adv. Energy Mater.* **2019**, *9*, 1902675.
[53] M. He, R. Guo, G. M. Hobold, H. Gao, B. M. Gallant, *PNAS* **2020**, *117*, 73–79.
[54] M. A. Hope, B. L. D. Rinkel, A. B. Gunnarsdóttir, K. Märker, S. Menkin, S. Paul, I. V. Sergeyev, C. P. Grey, *Nat. Commun.* **2020**, *11*, 2224.
[55] a) X. Cao, X. Ren, L. Zou, M. H. Engelhard, W. Huang, H. Wang, B. E. Matthews, H. Lee, C. Niu, B. W. Arey, Y. Cui, C. Wang, J. Xiao, J. Liu, W. Xu, J.-G. Zhang, *Nat. Energy* **2019**, *4*, 796–805; b) Z. Yu, H. Wang, X. Kong, W. Huang, Y. Tsao, D. G. Mackanic, K. Wang, X. Wang, W. Huang, S. Choudhury, Y. Zheng, C. V. Amanchukwu, S. T. Hung, Y. Ma, E. G. Lomeli, J. Qin, Y. Cui, Z. Bao, *Nat. Energy* **2020**, *5*, 526–533.
[56] J. Maier, *Adv. Funct. Mater.* **2011**, *21*, 1448–1455.
[57] C. Monroe, J. Newman, *J. Electrochem. Soc.* **2005**, *152*, A396.
[58] a) C. Pfaffenhuber, M. Göbel, J. Popovic, J. Maier, *Phys. Chem. Chem. Phys.* **2013**, *15*, 18318–18335; b) Z. Zhang, Y. Shao, B. Lotsch, Y.-S. Hu, H. Li, J. Janek, L. F. Nazar, C.-W. Nan, J. Maier, M. Armand, L. Chen,

*Energy Environ. Sci.* **2018**, *11*, 1945–1976; c) Z. Hu, G. Li, A. Wang, J. Luo, X. Liu, *Batteries & Supercaps*. **2020**, *3*, 331–335.
[59] C. Hou, J. Han, P. Liu, C. Yang, G. Huang, T. Fujita, A. Hirata, M. Chen, *Adv. Energy Mater.* **2019**, *9*, 1902675.
[60] L. Frenck, G. K. Sethi, J. A. Maslyn, N. P. Balsara, *Front. Energy Res.* **2019**, *7*.
[61] T. Zhu, Q. Hu, G. Yan, J. Wang, Z. Wang, H. Guo, X. Li, W. Peng, *Energy Technol.* **2019**, *7*, 1900273.
[62] a) J. Liu, Z. Bao, Y. Cui, E. J. Dufek, J. B. Goodenough, P. Khalifah, Q. Li, B. Y. Liaw, P. Liu, A. Manthiram, Y. S. Meng, V. R. Subramanian, M. F. Toney, V. V. Viswanathan, M. S. Whittingham, J. Xiao, W. Xu, J. Yang, X.-Q. Yang, J.-G. Zhang, *Nat. Energy* **2019**, *4*, 180–186; b) C. Fang, X. Wang, Y. Meng, *Trends Chem.* **2019**, pp. 152–158; c) S. Chen, C. Niu, H. Lee, Q. Li, L. Yu, W. Xu, J.-G. Zhang, E. J. Dufek, M. S. Whittingham, S. Meng, J. Xiao, J. Liu, *Joule* **2019**, *3*, 1094–1105; d) X.-B. Cheng, C. Yan, J.-Q. Huang, P. Li, L. Zhu, L. Zhao, Y. Zhang, W. Zhu, S.-T. Yang, Q. Zhang, *Energy Storage Mater.* **2017**, *6*, 18–25.
[63] S. C. Nagpure, T. R. Tanim, E. J. Dufek, V. V. Viswanathan, A. J. Crawford, S. M. Wood, J. Xiao, C. C. Dickerson, B. Liaw, *J. Power Sources* **2018**, *407*, 53–62.
[64] a) Y. Gao, M. Guo, K. Yuan, C. Shen, Z. Ren, K. Zhang, H. Zhao, F. Qiao, J. Gu, Y. Qi, K. Xie, B. Wei, *Adv. Energy Mater.* **2020**, *10*, 1903362; b) X.-Q. Zhang, T. Li, B.-Q. Li, R. Zhang, P. Shi, C. Yan, J.-Q. Huang, Q. Zhang, *Angew. Chem. Int. Ed. Engl.* **2020**, *59*, 3252–3257.
[65] P. Shi, X.-B. Cheng, T. Li, R. Zhang, H. Liu, C. Yan, X.-Q. Zhang, J.-Q. Huang, Q. Zhang, *Adv. Mater.* **2019**, *31*, 1902785.
[66] a) C. Niu, H. Lee, S. Chen, Q. Li, J. Du, W. Xu, J.-G. Zhang, M. S. Whittingham, J. Xiao, J. Liu, *Nat. Energy* **2019**, *4*, 551–559; b) L. Huang, J. Li, B. Liu, Y. Li, S. Shen, S. Deng, C. Lu, W. Zhang, Y. Xia, G. Pan, X. Wang, Q. Xiong, X. Xia, J. Tu, *Adv. Funct. Mater.* **2020**, *30*, 1910375.
[67] S. Jiao, J. Zheng, Q. Li, X. Li, M. H. Engelhard, R. Cao, J.-G. Zhang, W. Xu, *Joule* **2018**, *2*, 110–124.
[68] A. J. Louli, M. Genovese, R. Weber, S. G. Hames, E. R. Logan, J. R. Dahn, *J. Electrochem. Soc.* **2019**, *166*, A1291-A1299.
[69] X. Zhang, Q. J. Wang, K. L. Harrison, K. Jungjohann, B. L. Boyce, S. A. Roberts, P. M. Attia, S. J. Harris, *J. Electrochem. Soc.* **2019**, *166*, A3639-A3652.
[70] a) M. Mohammadi, E. V. Silletta, A. J. Ilott, A. Jerschow, *J. Magn. Reson.* **2019**, *309*, 106601; b) S. V. Erhard, P. J. Osswald, P. Keil, E. Höffer, M. Haug, A. Noel, J. Wilhelm, B. Rieger, K. Schmidt, S. Kosch, F. M. Kindermann, F. Spingler, H. Kloust, T. Thoennessen, A. Rheinfeld, A. Jossen, *J. Electrochem. Soc.* **2017**, *164*, A6324-A6333; c) T. C. Bach, S. F. Schuster, E. Fleder, J. Müller, M. J. Brand, H. Lorrmann, A. Jossen, G. Sextl, *J. Energy Storage* **2016**, *5*, 212–223.

Manuscript received: October 30, 2020
Revised manuscript received: January 15, 2021
Version of record online: February 12, 2021